ATP Hydrolysis Promotes Interactions between the Extracellular Ends of Transmembrane Segments 1 and 11 of Human Multidrug Resistance P-Glycoprotein†

Tip W. Loo, M. Claire Bartlett, and David M. Clarke*

Department of Medicine and Department of Biochemistry, University of Toronto, Toronto, Ontario, M5S 1A8, Canada

Received April 18, 2005; Revised Manuscript Received May 22, 2005

ABSTRACT: P-glycoprotein (P-gp, ABCB1) actively pumps a broad range of structurally unrelated cytotoxic compounds out of the cell. It has two homologous halves that are joined by a linker region. Each half has a transmembrane (TM) domain containing six TM segments and a nucleotide-binding domain (NBD). Cross-linking studies have shown that the drug-binding pocket is at the interface between the TM domains. The two NBDs interact to form the ATP-binding sites. Coupling of ATP hydrolysis to drug efflux has been postulated to occur by conversion of the binding pocket from a high-affinity to a low-affinity state through alterations in the packing of the TM segments. TM 11 has also been reported to be important for drug binding. Here, we used cysteine-scanning mutagenesis and oxidative cross-linking to test for changes in the packing of TM 11 during ATP hydrolysis. We generated 350 double cysteine mutants that contained one cysteine at the extracellular end of TM11 and another cysteine at the extracellular ends of TMs 1, 3, 4, 5, or 6. The mutants were expressed in HEK293 cells and treated with oxidant in the absence or presence of ATP. Cross-linked product was not detected in SDS−PAGE gels in the absence of ATP. By contrast, cross-linked product was detected in mutants M68C(TM1)/Y950C(TM11), M68C(TM1)/Y953C(TM11), M68C(TM1)/A954C(TM11), M69C(TM1)/A954C(TM11), and M69C(TM1)/ F957C(TM11) in the presence of ATP but not with ADP or AMP.PNP. These results indicate that rearrangement of TM11 may contribute to the release of drug substrate during ATP hydrolysis.

The human multidrug resistance P-glycoprotein (P-gp,[1] ABCB1) is an ATP-dependent drug pump that extracts cytotoxic compounds from the lipid bilayer and extrudes them into the extracellular medium (*1*). P-gp is a 170 kDa plasma membrane protein and is expressed in relatively high levels in the apical membranes of epithelial cells of intestine, kidney, liver, and blood−brain/testes barriers (*2*). The physiological role of P-gp is unknown. Its function may be to protect us from cytotoxic compounds in our diets and environment (*3*). Studies on knock-out mice show that P-gp is not essential for viability or reproduction but the mice demonstrate hypersensitivity to cytotoxic compounds (*4*). P-gp is clinically important because of its ability to compromise cancer and AIDS/HIV chemotherapies (*1, 5*).

P-gp is a member of the ATP-binding cassette (ABC) family of transporters (48 human members) (*6*). Its 1280 amino acids are organized as two homologous halves that are joined by a linker region (*7*). Each half begins with a transmembrane domain (TMD) containing six transmembrane (TM) segments followed by a hydrophilic nucleotide-binding domain (NBD).

There has been considerable progress made in characterizing the ATP-binding sites. Both NBDs are capable of hydrolyzing ATP (*8, 9*), but inhibition of either site inactivates the protein (*9*−*11*). Therefore, it has been proposed that ATP hydrolysis occurs via an alternating mechanism (*12*). The two ATP molecules bind at the interface between the Walker A sites and LSGGQ consensus sites of the NBDs (*13*−*15*), and drug substrates that stimulate or inhibit ATPase activity cause these sequences to come closer or move apart, respectively (*16*).

Drug substrates have been shown to bind at the interface between the two TMDs (*17*−*21*). Indeed, a truncated P-gp lacking both NBDs retained the ability to bind drug substrates (*22*). The results from several studies suggest that P-gp may have up to four distinct binding sites and that each substrate has a distinct binding site (*23*−*25*). In contrast, it has been proposed that P-gp has a common drug-binding pocket at the interface between the TMDs. In this model of drug binding, the broad range of structurally unrelated compounds that can be transported by P-gp may be explained by the "substrate-induced fit" mechanism (*20, 26*). Under this scenario, a substrate would create its own binding site by

† This work was supported by grants from the National Cancer Institute of Canada through the Canadian Cancer Society and from the Canadian Institutes of Health Research. D.M.C. is the recipient of the Canada Research Chair in Membrane Biology.

* Author to whom correspondence should be addressed. Mailing address: Department of Medicine, University of Toronto, Rm. 7342, Medical Sciences Building, 1 King's College Circle, Toronto, Ontario, M5S 1A8, Canada. Tel. or fax: 416-978-1105. E-mail: david.clarke@utoronto.ca.

[1] Abbreviations: P-gp, P-glycoprotein; NBD, nucleotide-binding domain; TMD, transmembrane domain; TM, transmembrane; HEK, human embryonic kidney; SDS−PAGE, sodium dodecyl sulfate−polyacrylamide gel electrophoresis.

10.1021/bi050705j CCC: $30.25
Published on Web 07/07/2005

using various combinations of residues from different TMs to form a particular binding site. The combination of residues involved in binding a particular substrate would determine the affinity for the substrate. Also, it is likely that some structurally different substrates may share the same residues during binding.

An important step in determining the mechanism of P-gp is to understand how ATP hydrolysis is coupled to drug efflux. It has been shown that TM6 and TM12 can undergo rotation or tilting during ATP hydrolysis (*27*−*29*) and that vanadate trapping of nucleotide exposes different residues of TM6 to the drug-binding pocket (*30*).

Another TM segment that is predicted to participate in ATP-dependent conformational changes is TM11 because it contributes residues to the common drug-binding pocket (*31, 32*) and likely forms part of the gating mechanism that allows drug substrates into the drug-binding pocket (*33*). In this study, we used cysteine-scanning mutagenesis and disulfide cross-linking analysis to test for ATP-dependent conformational changes between TM 11 in TMD2 and TMs 1, 3, 4, 5, and 6 in TMD1.

MATERIALS AND METHODS

Construction of Mutants. Cysteine-less P-gp was constructed by replacing the seven endogenous cysteines at positions 137, 431, 717, 956, 1074, 1125, and 1227 with alanines (*34, 35*). Double cysteine mutants were constructed by introducing a cysteine at the extracellular end of TM11 (positions 948−957) and another at the extracellular ends of TM1 (positions 66−72), TM3 (positions 204−210), TM4 (positions 213-219), TM5 (positions 309−315), or TM6 (positions 332−338). All of the mutants contained a 10-histidine tag at the COOH-end that facilitated purification of the mutant P-gp by nickel-chelate chromatography (*36*).

Disulfide Cross-Linking Analysis. The mutant P-gps were transiently expressed in human embryonic kidney (HEK) 293 cells as described previously (*37*). The cells were harvested and washed three times with phosphate-buffered saline (PBS, 10 mM sodium phosphate, pH 7.4, 150 mM NaCl) and the membranes prepared as described previously (*38*). The membranes were suspended in Tris-buffered saline (TBS, 10 mM Tris-HCl, pH 7.4, 150 mM NaCl).

For cross-linking, membranes were added to an equal volume of 2X ATPase buffer (100 mM Tris-HCl, pH 7.5, 100 mM NaCl, 20 mM $MgCl_2$, 2 mM ouabain, 4 mM EGTA, and 10 mM sodium azide) containing 10 mM ATP, 10 mM ADP, 10 mM AMP.PNP, or no nucleotide and incubated in an ice bath for 20 min. The samples were then treated with 1 mM oxidant (Cu^{2+}(phenanthroline)$_3$) for 10 min at 37 °C. To test for the effect of drug substrates on cross-linking, the membranes were preincubated with no drug substrate or with saturating concentrations of colchicine (10 mM), cyclosporin A (0.05 mM), verapamil (1 mM), or vinblastine (0.1 mM) for 15 min at 20 °C. The membranes were then mixed with one volume of 2X ATPase buffer containing 5 mM ATP and with or without 1 mM oxidant. The mixtures were incubated for 10 min at 37 °C and the reactions stopped by addition of 2XSDS sample buffer (125 mM Tris-HCl, pH 6.8, 20% (v/v) glycerol, and 4% (w/v) SDS) containing 50 mM EDTA and no reducing agent. The reaction mixtures were then subjected to SDS−PAGE (7.5% polyacrylamide gels) and immunoblot analysis with a rabbit polyclonal antibody against P-gp (*39*). Intramolecular disulfide cross-linking can be detected because the cross-linked product migrates with slower mobility on SDS−PAGE gels (*40*).

To test for the effect of vanadate trapping of nucleotide on cross-linking, the membranes were suspended in TBS and then preincubated for 15 min at 37 °C with an equal volume of 2X ATPase buffer containing 10 mM ATP, 20 mM $MgCl_2$, and 0.2 mM sodium vanadate. Sodium vanadate was boiled for 3 min to break polymeric species (*41*). The reaction mixtures were then treated with 1 mM oxidant for 10 min at 37 °C. The reactions were stopped by addition of 2XSDS sample buffer (125 mM Tris-HCl, pH 6.8, 20% (v/v) glycerol, and 4% (w/v) SDS) containing 50 mM EDTA and no reducing agent. The reaction mixtures were then subjected to SDS−PAGE (7.5% polyacrylamide gels) and immunoblot analysis with a rabbit polyclonal antibody against P-gp.

Isolation of P-gp Mutants and Measurement of Drug-Stimulated ATPase Activity. Fifty plates (10 cm diameter) of HEK 293 cells were transfected with mutant cDNA. After 24 h at 37 °C, the medium was replaced with fresh medium containing 10 μM cyclosporin A. Cyclosporin A, a substrate of P-gp, acts as a specific chemical (pharmacological) chaperone to increase the yield of mature P-gp by promoting proper folding of the molecule (*42*−*44*). After another 24 h at 37 °C, the cells were harvested, washed three times with PBS, and suspended in PBS. The cells were solubilized by addition of one volume of PBS containing 2% (w/v) *n*-dodecyl-β-D-maltoside. After 15 min at 4 °C, insoluble material was removed by centrifugation at 16000*g* for 15 min at 4 °C. The supernatant was passed through a DNA miniprep column (Qiagen Inc., Mississauga, Ontario) to remove DNA that inhibits flow through the nickel-chelate column. The flow-through material was then subjected to nickel-chelate chromatography as described previously (*36*).

An aliquot of the isolated histidine-tagged P-gp was then mixed with an equal volume of 10 mg/mL sheep brain phosphatidylethanolamine (type II-S, Sigma) that had been washed and suspended in TBS. The P-gp/lipid mixture was then sonicated, and a sample of the mixture was incubated with an equal volume of 2X ATPase buffer containing 10 mM ATP with and without 1 mM verapamil. Verapamil was selected because it is a P-gp substrate that highly stimulates the ATPase activity of P-gp (*32*). The samples were incubated for 30 min at 37 °C, and the amount of inorganic phosphate released was determined (*45*).

RESULTS

Previous studies have shown that, in the absence of ATP, the drug-binding pocket is "funnel-shaped": "closed" at the cytoplasmic end, at least 9−25 Å in the middle, and wider still at the extracytoplasmic side (*19, 46*). Figure 1A shows the predicted orientation of the twelve TM segments of P-gp in the absence of ATP. It has been shown that TMs 4, 5, and 6 in TMD1 and TMs 9, 10, 11, and 12 in TMD2 contribute residues to the common drug-binding pocket of P-gp (*17*−*21, 32, 47*).

TM11 lies next to TM 2 because cysteines introduced into TMs 2 and11 can be cross-linked at the cytoplasmic side

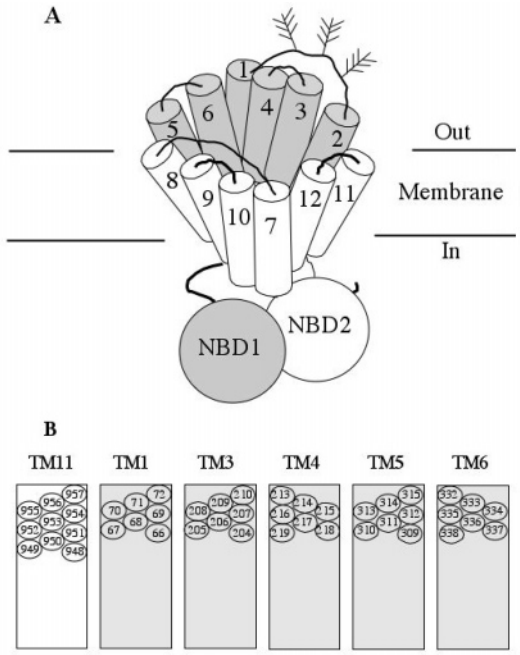

FIGURE 1: Model of packing of the TM segments of P-gp and location of the introduced cysteines. (A) Model of the organization of the of the TM segments (numbered) surrounding the common drug-binding pocket. The first half of P-gp is shown in gray, and the second half is shown in white. The branched lines between TMs 1 and 2 represent glycosylation sites. NBD1 and NBD2 represent the first and second nucleotide-binding domains, respectively. (B) The positions of the introduced cysteine residues at the extracellular ends of TMs 11, 1, 3, 4, 5, and 6 in TMD1 are shown in the ovals. The TMs in the second half of P-gp are shaded in gray.

with a zero-length cross-linker (*48*) or at the extracellular side with a 6−16 Å cross-linker (*49*). TM11 may be a particularly important TM because its residues contribute to drug-binding (*32*) and it may be part of the gate into the drug-binding pocket (*33*). TM11 is also predicted to be adjacent to TM 12 and is attached to TM12 by an extracellular loop of 16 residues (positions 958−973). It has been shown that TM12 (L975C) approaches TM6 (L332C) on the extracellular side during ATP hydrolysis (*27*). Therefore, we wanted to test whether TM 11 also showed conformational changes during ATP hydrolysis. The rationale is that since TM 11 is at the end of the drug-binding pocket, changes in its conformation during ATP hydrolysis will provide insight into how the shape of the drug-binding pocket changes during the transport cycle. Accordingly, we constructed 350 double mutants by introducing a cysteine at the extracellular end of TM11 (positions 948−957) and another at the extracellular ends of TM1 (positions 66−72), TM3 (positions 204−210), TM4 (positions 213-219), TM5 (positions 309−315), or TM6 (positions 332−338) of a histidine-tagged Cys-less P-gp (Figure 1B). The Cys-less mutant of P-gp is a valuable tool because it shows robust activity (*35*) and introduction of cysteines into most positions in the TM segments does not inhibit activity or cause misprocessing of the mutant (*18*). TM2 was omitted as we previously showed that cysteines in TM2 could be cross-linked to cysteines in TM11 in the absence of ATP (*48*). The 350 double cysteine mutants were transiently expressed in HEK 293 cells. Membranes were prepared and then treated with or without 1 mM oxidant for 10 min at 37 °C in the presence or absence of 5 mM ATP. To reduce the activity of other ATPases, ouabain, EGTA, and sodium azide were included in the reaction mixtures. The reactions were stopped by addition of SDS sample buffer containing 50 mM EDTA and no reducing agent. The samples were subjected to SDS−PAGE and immunoblot analysis. Disulfide cross-linking analysis is a useful technique because cross-linking of cysteines in different domains causes the protein to migrate with slower mobility in nonreducing SDS−PAGE gels (*40*). In the absence of ATP, cross-linked product was not detected in any of the 350 double cysteine mutants (data not shown). In the presence of ATP, however, cross-linked product was detected in five mutants, M68C(TM1)/Y950C(TM11), M68C(TM1)/Y953C(TM11), M68C(TM1)/A954C(TM11), M69C(TM1)/A954C(TM11), and M69C(TM1)/ F957C(TM11) (Figure 2A). The other 345 double cysteine mutants did not show ATP-dependent cross-linking. A representative negative mutant, F72C(TM1)/ F957C(TM11), is shown in Figure 2A.

To confirm that the slower migrating products in mutants M68C(TM1)/Y950C(TM11), M68C(TM1)/Y953C(TM11), M68C(TM1)/A954C(TM11), M69C(TM1)/A954C(TM11), and M69C(TM1)/F957C(TM11) after treatment with oxidant in the presence of ATP were indeed due to the formation of an intramolecular disulfide bond, the cross-linked mutants were subjected to treatment with the reducing agent, dithiothreitol. Figure 2A shows that the slower migrating product in mutants M68C(TM1)/Y950C(TM11), M68C-(TM1)/Y953C(TM11), M68C(TM1)/A954C(TM11), M69C-(TM1)/A954C(TM11), and M69C(TM1)/F957C(TM11) was greatly reduced upon exposure to 10 mM dithiothreitol. This would be consistent with the presence of a disulfide bond in these mutants. To rule out the possibility that the cross-linked product in mutants M68C(TM1)/Y950C(TM11), M68C(TM1)/ Y953C(TM11), M68C(TM1)/A954C(TM11), M69C(TM1)/ A954C(TM11), and M69C(TM1)/F957C(TM11) was due to disulfide formation between P-gp molecules, we expressed the single mutants M68C(TM1), M69C(TM1), Y950C(TM11), Y953C(TM11), A954C(TM11), or F957C(TM11) alone. In addition, pairs of cDNAs coding for single cysteine mutants were cotransfected into HEK 293 cells. Membranes were then prepared from transfected cells and subjected to oxidative cross-linking for 10 min at 37 °C in the presence or absence of 5 mM ATP. Figure 2B shows that cross-linked product was not detected when the single cysteine mutants M68C(TM1), M69C(TM1), Y950C(TM11), Y953C(TM11), A954C(TM11), or F957C(TM11) were expressed. Similarly, no cross-linked product was detected when pairs of single cysteine mutants M68C(TM1) plus Y950C(TM11), M68C(TM1) plus Y953C(TM11), M68C(TM1) plus A954C(TM11), M69C(TM1) plus A954C(TM11), or M69C(TM1) plus F957C(TM11) were coexpressed (Figure 2C). Therefore, the slower migrating species seen in mutants M68C(TM1)/Y950C(TM11), M68C(TM1)/Y953C(TM11), M68C(TM1)/A954C(TM11), M69C(TM1)/A954C(TM11), and M69C(TM1)/F957C(TM11) (Figure 2A) were due to intramolecular cross-linking and not due to cross-linking between two individual P-gp molecules.

We then monitored the time dependence of cross-linking in the presence or absence of ATP. Mutants M68C(TM1)/ Y950C(TM11), M68C(TM1)/Y953C(TM11), M68C(TM1)/ A954C(TM11), M69C(TM1)/A954C(TM11), and M69C-(TM1)/F957C(TM11) all showed a time-dependent increase

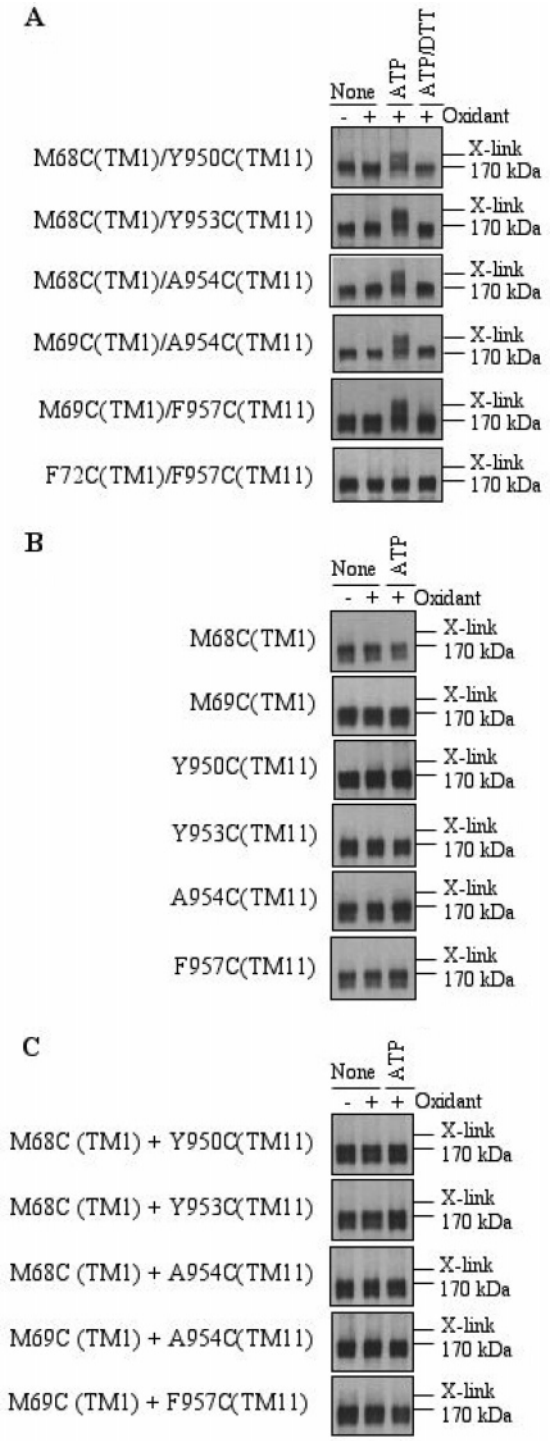

FIGURE 2: Disulfide cross-linking of P-gp mutants. Membranes were prepared from HEK 293 cells (A), expressing mutants M68C(TM1)/Y950C(TM11), M68C(TM1)/Y953C(TM11), M68C(TM1)/A954C(TM11), M69C(TM1)/A954C(TM11), M69C(TM1)/F957C(TM11), or the negative mutant F72C(TM1)/F957C(TM11); (B) the single cysteine mutants M68C(TM1), M69C(TM1), Y950C(TM11), Y953C(TM11), A954C(TM11), or F957C(TM11); or (C) coexpressing the single cysteine mutants M68C(TM1) plus Y950C(TM11), M68C(TM1) plus Y953C(TM11), M68C(TM1) plus A954C(TM11), M69C(TM1) plus A954C(TM11), or M69C(TM1) plus F957C(TM11). The membranes were treated without (−) or with (+) oxidant in the presence of ATP. A sample that was cross-linked in the presence of ATP was also treated with dithiothreitol (ATP/DTT) (A). The reactions were stopped by addition of SDS sample buffer containing EDTA and subjected to immunoblot analysis. The positions of the cross-linked (X-link) and mature (170 kDa) P-gps are indicated.

FIGURE 3: Time-dependent cross-linking of mutant M69C(TM1)/A954C(TM11). Membranes were prepared from HEK 293 cells expressing mutant M69C(TM1)/A954C(TM11). The membranes were treated with 1 mM oxidant at 37 °C for various times (min) in the presence (+ ATP) or absence (− ATP) of 5 mM ATP. The reactions were stopped by addition of SDS sample buffer containing EDTA and subjected to immunoblot analysis. The positions of the cross-linked (X-link) and mature (170 kDa) P-gps are indicated.

in the amount of cross-linked product. The results observed in mutant M69C(TM1)/A954C(TM11) are shown as an example (Figure 3). When mutant M69C(TM1)/A954C(TM11) was treated with 1 mM oxidant at 37 °C in the absence of ATP, only low levels of cross-linked product were observed at the longest interval (16 min). When the mutant was cross-linked in the presence of 5 mM ATP, however, cross-linked product was detected within 1 to 2 min. By 16 min, about 50% of the P-gp was cross-linked. Higher levels of cross-linking may be limited by the orientation of the membrane vesicles and accessibility of the ATP-binding sites to ATP. The rate of cross-linking is lower than the rate of ATP hydrolysis. This may be because during ATP hydrolysis the cross-linkable cysteines come together very transiently while the cross-linking step likely requires more time. Therefore, the cross-linked state may represent only a small proportion of these transient conformations.

We then determined whether cross-linking was enhanced by ATP hydrolysis or by binding of nucleotides. Mutant M69C(TM1)/A954C(TM11) membranes were preincubated for 20 min at 4 °C with or without 5 mM ATP, 5 mM ADP, or the nonhydrolyzable ATP analogue, AMP.PNP, and then treated with 1 mM oxidant for 10 min at 37 °C. The reaction was stopped by addition of SDS sample buffer containing EDTA and no reducing agent. The samples were subjected to SDS−PAGE and immunoblot analysis. Figure 4 shows that a substantial amount of cross-linked product was detected only with ATP. Little cross-linked product was detected in the presence of ADP or AMP.PNP. Similar results were obtained with mutants M68C(TM1)/Y950C(TM11), M68C(TM1)/Y953C(TM11), M68C(TM1)/A954C(TM11), and M69C(TM1)/F957C(TM11) (data not shown). It should be pointed out that the enzyme is trapped in a fixed state with nonhydrolyzable nucleotides (ADP or AMP.PNP). Under turnover conditions, however, there may be many active conformations of the enzyme. Therefore, cross-linking could occur at any of these steps and not necessarily at the hydrolytic step.

Next, we tested whether cross-linking was affected when P-gp is trapped in a transition state using vanadate (*50*). Vanadate traps ADP at either NBD by mimicking the transition state of the γ-phosphate of ATP during ATP hydrolysis. Vanadate trapping at one NBD inhibits hydrolysis at the second site (*50*). Accordingly, membranes were prepared from HEK 293 cells expressing mutant M69C(TM1)/A954C(TM11) and preincubated with ATP plus vanadate for 15 min at 37 °C to promote vanadate trapping of nucleotide. Incubation of P-gp under such conditions causes

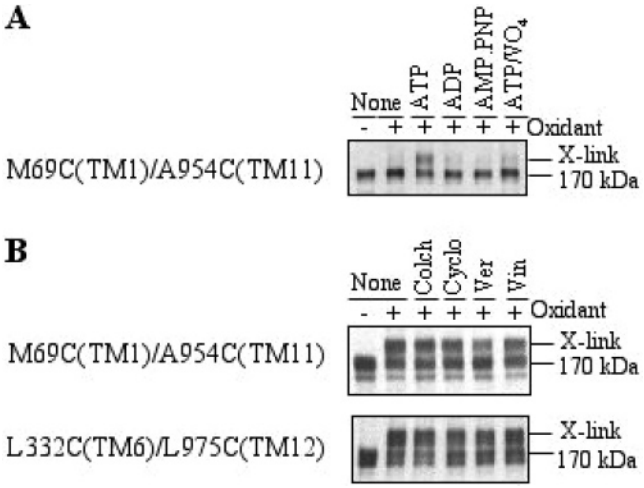

FIGURE 4: Effect of nucleotides, vanadate trapping of nucleotide, and drug substrates on cross-linking of mutants. (A) Membranes from HEK 293 cells expressing mutant M69C(TM1)/A954C(TM11) were preincubated on ice for 20 min in ATPase buffer containing 5 mM ATP, 5 mM ADP, 5 mM AMP.PNP, or no nucleotide (None). The samples were then treated with (+) or without (−) oxidant for 15 min at 37 °C. For vanadate tapping of nucleotide, membranes were incubated in ATPase buffer containing 5 mM ATP plus 0.2 mM sodium vanadate (ATP/VO_4). The membranes were then treated with 1 mM oxidant for 15 min at 37 °C in the presence of 5 mM ATP. (B) Membranes prepared from HEK 293 cells expressing mutant M69C(TM1)/A954C(TM11) or mutant L332C-(TM6)/L975C(TM12) were preincubated with 10 mM colchicine (Colch), 0.05 mM cyclosporin A (Cyclo), 1 mM verapamil (Ver), 0.1 mM vinblastine (Vin), or no drug substrate (None) for 15 min at 20 °C. The samples were then incubated with buffer containing 5 mM ATP and with (+) or without (−) oxidant for 10 min at 37 °C. The reactions were stopped by addition of SDS sample buffer containing EDTA and subjected to immunoblot analysis. The positions of the cross-linked (X-link) and mature (170 kDa) P-gps are indicated.

>90% inhibition of P-gp ATPase activity (*28*). Inhibition of P-gp by vanadate is long-lived with a half-life of 84 min at 37 °C (*50*). The samples were then treated with oxidant for 10 min at 37 °C. Figure 4A shows that vanadate trapping of nucleotide inhibited cross-linking. Similar results were obtained with mutants M68C(TM1)/Y950C(TM11), M68C(TM1)/Y953C(TM11), M68C(TM1)/A954C(TM11), and M69C(TM1)/F957C(TM11) (data not shown). Therefore, it appears that conditions in which the enzyme does not turn over (with no nucleotide, ADP, AMP.PNP, or ATP plus vanadate) all resulted in low levels of cross-linking.

We previously showed that the presence of drug substrate completely inhibited disulfide cross-linking between cysteines introduced at the intracellular ends of TM6 and TM12 (*27*). For example, cross-linking between G346C(TM6) and G989C(TM12) with oxidant was completely inhibited in the presence of drug substrates colchicine, cyclosporin A, verapamil, or vinblastine. Therefore, we were interested in determining whether the presence of drug substrate also affected cross-linking between cysteine residues at the extracellular ends of the TM segments in TMD1 and TMD2, respectively. Accordingly, membranes were prepared from HEK 293 cells expressing mutants M69C(TM1)/A954C(TM11) or mutant L332C(TM6)/L975C(TM12). The cysteine residues in mutant L332C(TM6)/L975C(TM12) are at the extracellular ends of TM6 and TM12, respectively, and the mutant was also cross-linked with oxidant during

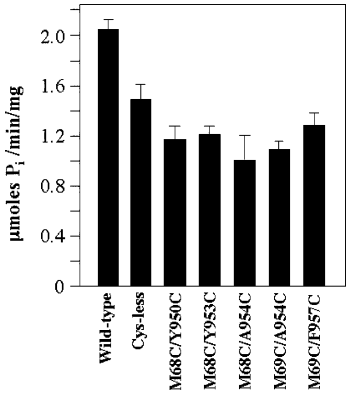

FIGURE 5: Verapamil-stimulated ATPase activities of P-gp mutants. Histidine-tagged wild-type, Cys-less, and P-gp mutants M68C-(TM1)/Y950C(TM11), M68C(TM1)/Y953C(TM11), M68C(TM1)/A954C(TM11), M69C(TM1)/A954C(TM11), or M69C(TM1)/F957C(TM11) were expressed in HEK 293 cells. The cells were harvested and solubilized with *n*-dodecyl-*β*-D-maltoside, and histidine-tagged P-gp was isolated by nickel-chelate chromatography. Equivalent amounts of P-gp were mixed with lipids and sonicated, and ATPase activity was measured in the presence of 1 mM verapamil. Each value is the average of triplicate determinations.

ATP hydrolysis (*27*). The membranes were then incubated with colchicine, cyclosporin A, verapamil, or vinblastine for 15 min at 20 °C and then treated with oxidant in the presence or absence of ATP. The reactions were stopped by addition of sample buffer and then subjected to immunoblot analysis. In the absence of ATP, the drug substrates colchicine, cyclosporin A, verapamil, or vinblastine did not cause cross-linking of the mutants (data not shown). In the presence of ATP and substrate, however, cross-linked product was still detected in both mutants M69C(TM1)/A954C(TM11) and L332C(TM6)/L975C(TM12) (Figure 4B). These results indicate that ATP hydrolysis caused disulfide cross-linking between the extracellular ends of TMs 1/11 and 6/12 in the presence or absence of drug substrate.

Finally, we tested whether mutants M68C(TM1)/Y950C-(TM11), M68C(TM1)/Y953C(TM11), M68C(TM1)/A954C-(TM11), M69C(TM1)/A954C(TM11), and M69C(TM1)/F957C(TM11) that showed ATP-dependent cross-linking were still active. We monitored the activities of these mutants by measuring verapamil-stimulated ATPase activity. Drug substrates stimulate the ATPase activity of P-gp about 2−20-fold (*16*). Verapamil was selected because it is one of the best stimulators of P-gp ATPase activity (*32*). It has also been demonstrated that there is a good correlation between drug stimulation of ATPase activity and drug transport (*51*). Accordingly, the histidine-tagged P-gp mutants M68C(TM1)/Y950C(TM11), M68C(TM1)/Y953C(TM11), M68C(TM1)/A954C(TM11), M69C(TM1)/A954C(TM11), and M69C-(TM1)/F957C(TM11) and the Cys-less P-gp were expressed in HEK 293 cells and isolated by nickel-chelate chromatography. The isolated P-gps were mixed with lipid, sonicated, and assayed for verapamil-stimulated ATPase activity under saturating concentrations (1 mM verapamil). The Cys-less parent P-gp exhibited verapamil-stimulated ATPase activity of 1.47 μmol of P_i/min/(mg of protein) (Figure 5). The verapamil-stimulated ATPase activities of the mutants ranged from 1.01 to 1.32 μmol of P_i/min/(mg of protein). The relative activities were 81%, 82%, 69%, 77%, and 90% of Cys-less P-gp for mutants M68C(TM1)/Y950C(TM11),

M68C(TM1)/Y953C(TM11), M68C(TM1)/A954C(TM11), M69C(TM1)/A954C(TM11), and M69C(TM1)/F957C(TM11), respectively. These result show that the mutants were active and the presence of cysteines caused only a moderate decrease in the activity of the mutants.

DISCUSSION

The results in this study show that ATP hydrolysis causes a rearrangement of the TM segments such that cysteine residues at positions 68 and 69 in TM1 come close to cysteines at positions 950, 953, 954, and 957 in TM11. The effect of ATP on movement of TMs 1 and 11 may be better understood by arranging the TM1 and TM 11 residues in α-helices. As shown in Figure 6A, residues 68 and 69 are adjacent to each other on one face of TM11. Similarly, residues 950, 953, 954, and 957 in TM11 are on one face of TM11. Therefore, TMs 1 and 11 have reactive "patches" of residues that come close together during ATP hydrolysis and can be trapped through disulfide cross-linking. Cross-linking was quite specific because cross-linking was observed during ATP hydrolysis in only 5 of the 350 double cysteine mutants. Furthermore, no cross-linking was detected in the absence of ATP, when single cysteine mutants were expressed alone or when coexpressed (Figure 2B,C).

TM11 contributes residues to the drug-binding pocket because cysteines introduced into TM11 can be labeled with thiol-reactive drug substrate analogues such as dibromobimane and methanethiosulfonate (MTS)-verapamil (*18*, *32*). Labeling of residues F942C and T945C by these thiol-reactive drug substrate analogues was inhibited by the presence of drug substrate. Figure 6B shows that residues 942 and 945 are close to each other in the α-helical wheel but occupy a different face of the helix than the cross-linkable residues (positions 950, 953, 954, and 957). Residues at positions 942 and 945 in TM11 are located closer to the middle of the TM segments, and this would be more in concert with the idea that the drug substrates enter the lipid bilayer before entering the common drug-binding pocket of P-gp.

Detection of ATP-dependent conformational changes in TMs 1 and 11 may help explain how ATP hydrolysis leads to drug efflux. Drug substrates can bind P-gp with relatively high affinity even in the absence of both NBDs (*22*). It has been reported that the drug-binding site in P-gp changes from a high-affinity state to a low-affinity state during the transport cycle (*52*). Therefore, release of drug substrate will require a change in the conformation/rearrangement of the drug-binding pocket. The results from this study show that ATP hydrolysis may disrupt drug substrate interaction with TM11 by causing lateral movement or rotation of the TM as it approaches TM1. Such large conformational changes in the drug-binding pocket have also been detected in TM6 and TM12. Both TM6 and TM12 contribute residues to the common drug-binding pocket (*47*). In the presence of ATP, however, TM6 and TM12 can undergo rotation/lateral movement (*27*, *28*). This is supported by the results of Rothnie et al. (*29*), who showed that TM6 moves during the catalytic cycle. Similarly, vanadate trapping of nucleotide traps the drug-binding pocket in an altered conformation such that different residues of TM6 are exposed to the drug-binding pocket when compared to the resting state (*30*).

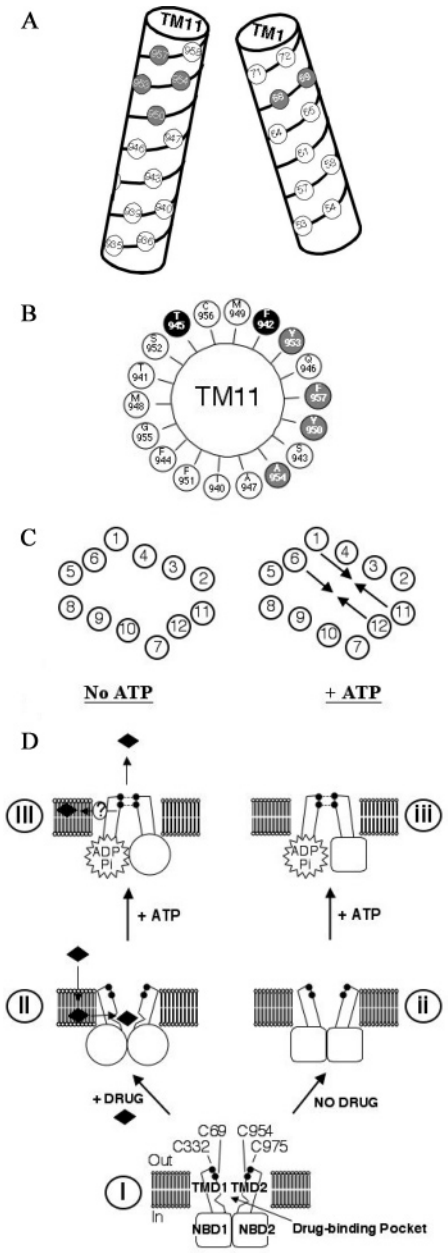

FIGURE 6: Models of disulfide cross-linking between TM1 and TM11. (A) The residues of TM1 and TM11 are arranged in α-helices. The cross-linkable cysteines (positions 68 and 69 in TM1, positions 950, 953, 954, and 957 in TM11) are indicated by the gray-filled circles. (B) The α-helical wheel arrangement of TM11 residues shows that the cross-linkable cysteines (gray-filled circles) and the thiol-reactive cysteines (black-filled circles) are on different faces of the helix. (C) Model showing ATP-induced conformational changes in P-gp. The numbered circles represent the extracellular ends of the TM segments. In the basal state, TM2 and TM11 are close together. In the presence of ATP, however, the extracellular ends of TM11 and TM12 approach those of TM1 and TM6, respectively (arrows), in a "scissor-like" movement. (D) Model of cross-linking at the extracellular ends of TM segments in TMD1 (Cys69(TM1) and Cys332(TM6)) and TMD2 (Cys954(TM11) and Cys975(TM12)). Under basal/uncoupled conditions (NO DRUG), the drug-binding pocket is predicted to be in a low-affinity state (state ii) (*56*). ATP hydrolysis in the uncoupled state results in rearrangement of the TM segments such that cross-linking is possible between Cys69(TM1)/Cys954(TM11) and Cys332(TM6)/Cys975(TM12) (state iii). In the coupled pathway (+ DRUG), the drug substrate binds to the high-affinity binding site (state II). ATP hydrolysis, however, causes similar rearrangement of the TMs resulting in cross-linking between the extracellular ends of TMs 1/11 and TMs 6/12 (state III) as observed in the uncoupled pathway.

The environment surrounding the disulfide bond in the TM6/TM12 double cysteine mutant, (L332C(TM6)/L975(TM12), must be quite different from the disulfide bonds formed between cysteines in TMs 1 and 11. The disulfide bond formed in the presence of ATP in mutant L332C(TM6)/L975(TM12) was insensitive to thiol reducing agents (100 mM dithiothreitol) (*27*). The cross-linked products in the TM1/TM11 mutants (Figure 2), however, could be reduced with 10 mM dithiothreitol. A possible explanation is that the TM1/TM11 but not the TM6/TM12 disulfide bonds are accessible to solvent. This would be consistent with the study showing that some residues in the common drug-binding pocket become more accessible to water during ATP hydrolysis (*53*).

Nucleotide-induced conformational changes in the TMDs of P-gp have also been detected using other approaches. Spectroscopic techniques have shown that P-gp undergoes global changes during substrate or nucleotide binding (*54*). Similarly, electron microscopy techniques have shown conformational changes during nucleotide binding (*55*). Rothnie et al. (*29*) used fluorescence-labeling techniques to show distinct labeling patterns for cysteines introduced into TM6 with hydrophobic or hydrophilic probes for P-gp in the basal, AMP.PNP bound, or ADP/vanadate trapped states. The results from these studies are consistent with the proposal that ATP binding and hydrolysis lead to release of drug substrates by causing major rearrangement of the TM segments within the drug-binding pocket.

The effects with ATP that were observed in the TM 1/11 mutants must occur during ATP hydrolysis since no detectable effect was observed with ADP or AMP.PNP. Hydrolysis of ATP appears to cause the TMDs to move past each other in a "scissor-like" fashion during rearrangement of the drug-binding pocket (Figure 6C).

Thermodynamic analyses of ATP hydrolysis in the absence or presence of drug substrates by Al-Shawi et al. (*56*) showed the presence of two distinct transition states for P-gp: one associated with uncoupled basal activity and the other with coupled drug transport. This suggests that, during ATP hydrolysis, P-gp undergoes different conformational states when in the drug-bound (coupled) and drug-free (uncoupled) states. In the present study, however, we observed cross-linking during ATP hydrolysis between the extracellular ends of TMs 1/11 and TMs 6/12 in the presence or absence of drug substrate (Figure 4B). One way to reconcile these results is that the TM 1/11 and TM 6/12 cross-linked products represent conformations that are common in the coupled and uncoupled pathways of P-gp. Similarly, inhibition of P-gp ATPase activity in the coupled or uncoupled state by *N*-ethylmaleimide suggests the presence of conformations that are common to both pathways (*11*). Therefore, it appears that major rearrangements of the TM segments occur in P-gp during the basal or transport pathways (Figure 6D).

There is no high-resolution structure available for P-gp. The crystal structure of a related bacterial ABC transporter from *Vibrio cholera*, MsbA, however, has been determined (*57*) and provides a framework for interpreting our results. MsbA is a complex of two identical polypeptides, each containing 6 TM segments and an ATP-binding domain. The protein transports lipid A out of the cell. The amino acid sequence of MsbA has 27% identity with that of P-gp. The structure of MsbA shows that the extracellular end of TM1 in one polypeptide is relatively close to that of TM5 (equivalent to TM11 in P-gp) of the second polypeptide. A more recent structure of MsbA in the vanadate-trapped state showed that TM1 and the loop connecting TMs 5 and 6 (equivalent to TMs 5/6 and TMs 11/12 in P-gp) had undergone significant rearrangement compared to the basal state (*58*). Therefore, the conformational changes observed in P-gp may be a common feature in the mechanism of other ABC transporters.

REFERENCES

1. Ambudkar, S. V., Dey, S., Hrycyna, C. A., Ramachandra, M., Pastan, I., and Gottesman, M. M. (1999) Biochemical, cellular, and pharmacological aspects of the multidrug transporter, *Annu. Rev. Pharmacol. Toxicol. 39*, 361−398.
2. Thiebaut, F., Tsuruo, T., Hamada, H., Gottesman, M. M., Pastan, I., and Willingham, M. C. (1987) Cellular localization of the multidrug-resistance gene product P-glycoprotein in normal human tissues, *Proc. Natl. Acad. Sci. U.S.A. 84*, 7735−7738.
3. Loo, T. W., and Clarke, D. M. (1999) Molecular Dissection of the Human Multidrug Resistance P-glycoprotein, *Biochem. Cell. Biol. 77*, 11−23.
4. Schinkel, A. H., Smit, J. J., van Tellingen, O., Beijnen, J. H., Wagenaar, E., van Deemter, L., Mol, C. A., van der Valk, M. A., Robanus-Maandag, E. C., te Riele, H. P., Berns, A. J. M., and Borst, P. (1994) Disruption of the mouse mdr1a P-glycoprotein gene leads to a deficiency in the blood-brain barrier and to increased sensitivity to drugs, *Cell 77*, 491−502.
5. Lee, C. G., Gottesman, M. M., Cardarelli, C. O., Ramachandra, M., Jeang, K. T., Ambudkar, S. V., Pastan, I., and Dey, S. (1998) HIV-1 protease inhibitors are substrates for the MDR1 multidrug transporter, *Biochemistry 37*, 3594−3601.
6. Dean, M., Rzhetsky, A., and Allikmets, R. (2001) The human ATP-binding cassette (ABC) transporter superfamily, *Genome Res. 11*, 1156−1166.
7. Chen, C. J., Chin, J. E., Ueda, K., Clark, D. P., Pastan, I., Gottesman, M. M., and Roninson, I. B. (1986) Internal duplication and homology with bacterial transport proteins in the mdr1 (P-glycoprotein) gene from multidrug-resistant human cells, *Cell 47*, 381−389.
8. Loo, T. W., and Clarke, D. M. (1994) Reconstitution of drug-stimulated ATPase activity following co- expression of each half of human P-glycoprotein as separate polypeptides, *J. Biol. Chem. 269*, 7750−7755.
9. Urbatsch, I. L., Sankaran, B., Bhagat, S., and Senior, A. E. (1995) Both P-glycoprotein nucleotide-binding sites are catalytically active, *J. Biol. Chem. 270*, 26956−26961.
10. Azzaria, M., Schurr, E., and Gros, P. (1989) Discrete mutations introduced in the predicted nucleotide-binding sites of the mdr1 gene abolish its ability to confer multidrug resistance, *Mol. Cell. Biol. 9*, 5289−5297.
11. Loo, T. W., and Clarke, D. M. (1995) Covalent modification of human P-glycoprotein mutants containing a single cysteine in either nucleotide-binding fold abolishes drug- stimulated ATPase activity, *J. Biol. Chem. 270*, 22957−22961.
12. Senior, A. E., and Gadsby, D. C. (1997) ATP hydrolysis cycles and mechanism in P-glycoprotein and CFTR, *Semin. Cancer Biol. 8*, 143−150.
13. Hopfner, K. P., Karcher, A., Shin, D. S., Craig, L., Arthur, L. M., Carney, J. P., and Tainer, J. A. (2000) Structural biology of Rad50 ATPase: ATP-driven conformational control in DNA double-strand break repair and the ABC-ATPase superfamily, *Cell 101*, 789−800.
14. Loo, T. W., Bartlett, M. C., and Clarke, D. M. (2002) The "LSGGQ" motif in each nucleotide-binding domain of human P-glycoprotein is adjacent to the opposing walker A sequence, *J. Biol. Chem. 277*, 41303−41306.
15. Fetsch, E. E., and Davidson, A. L. (2002) Vanadate-catalyzed photocleavage of the signature motif of an ATP-binding cassette (ABC) transporter, *Proc. Natl. Acad. Sci. U.S.A. 99*, 9685−9690.

16. Loo, T. W., Bartlett, M. C., and Clarke, D. M. (2003) Drug binding in human P-glycoprotein causes conformational changes in both nucleotide-binding domains, *J. Biol. Chem. 278*, 1575−1578.
17. Loo, T. W., and Clarke, D. M. (2000) Identification of residues within the drug-binding domain of the human multidrug resistance P-glycoprotein by cysteine-scanning mutagenesis and reaction with dibromobimane, *J. Biol. Chem. 275*, 39272−39278.
18. Loo, T. W., and Clarke, D. M. (2001) Defining the drug-binding site in the human multidrug resistance P-glycoprotein using MTS-verapamil. *J. Biol. Chem. 276*, 14972−14979.
19. Loo, T. W., and Clarke, D. M. (2001) Determining the dimensions of the drug-binding domain of human P-glycoprotein using thiol cross-linkers as molecular rulers, *J. Biol. Chem. 276*, 36877−36880.
20. Loo, T. W., and Clarke, D. M. (2002) Location of the rhodamine-binding site in the human multidrug resistance P-glycoprotein, *J. Biol. Chem. 277*, 44332−44338.
21. Pleban, K., Kopp, S., Csaszar, E., Peer, M., Hrebicek, T., Rizzi, A., Ecker, G. F., and Chiba, P. (2005) P-glycoprotein substrate binding domains are located at the transmembrane domain/transmembrane domain interfaces: a combined photoaffinity labeling-protein homology modeling approach, *Mol. Pharmacol. 67*, 365−374.
22. Loo, T. W., and Clarke, D. M. (1999) The transmembrane domains of the human multidrug resistance P-glycoprotein are sufficient to mediate drug binding and trafficking to the cell surface, *J. Biol. Chem. 274*, 24759−24765.
23. Dey, S., Ramachandra, M., Pastan, I., Gottesman, M. M., and Ambudkar, S. V. (1997) Evidence for two nonidentical drug-interaction sites in the human P-glycoprotein, *Proc. Natl. Acad. Sci. U.S.A. 94*, 10594−10599.
24. Pascaud, C., Garrigos, M., and Orlowski, S. (1998) Multidrug resistance transporter P-glycoprotein has distinct but interacting binding sites for cytotoxic drugs and reversing agents, *Biochem. J. 333*, 351−358.
25. Shapiro, A. B., Fox, K., Lam, P., and Ling, V. (1999) Stimulation of P-glycoprotein-mediated drug transport by prazosin and progesterone. Evidence for a third drug-binding site, *Eur. J. Biochem. 259*, 841−850.
26. Loo, T. W., Bartlett, M. C., and Clarke, D. M. (2003) Substrate-induced Conformational Changes in the Transmembrane Segments of Human P-glycoprotein. DIRECT EVIDENCE FOR THE SUBSTRATE-INDUCED FIT MECHANISM FOR DRUG BINDING, *J. Biol. Chem. 278*, 13603−13606.
27. Loo, T. W., and Clarke, D. M. (1997) Drug-stimulated ATPase activity of human P-glycoprotein requires movement between transmembrane segments 6 and 12, *J. Biol. Chem. 272*, 20986−20989.
28. Loo, T. W., and Clarke, D. M. (2001) Cross-linking of human multidrug resistance P-glycoprotein by the substrate, Tris-(2-maleimidoethyl)amine, is altered by ATP hydrolysis: Evidence for rotation of a transmembrane helix, *J. Biol. Chem. 276*, 31800−31805.
29. Rothnie, A., Storm, J., Campbell, J., Linton, K. J., Kerr, I. D., and Callaghan, R. (2004) The topography of transmembrane segment six is altered during the catalytic cycle of P-glycoprotein, *J. Biol. Chem. 279*, 34913−34921.
30. Loo, T. W., and Clarke, D. M. (2002) Vanadate trapping of nucleotide at the ATP-binding sites of human multidrug resistance P-glycoprotein exposes different residues to the drug-binding site, *Proc. Natl. Acad. Sci. U.S.A. 99*, 3511−3516.
31. Kajiji, S., Talbot, F., Grizzuti, K., Van Dyke-Phillips, V., Agresti, M., Safa, A. R., and Gros, P. (1993) Functional analysis of P-glycoprotein mutants identifies predicted transmembrane domain 11 as a putative drug binding site, *Biochemistry 32*, 4185−4194.
32. Loo, T. W., and Clarke, D. M. (1999) Identification of residues in the drug-binding domain of human P-glycoprotein: Analysis of transmembrane segment 11 by cysteine-scanning mutagenesis and inhibition by dibromobimane, *J. Biol. Chem. 274*, 35388−35392.
33. Loo, T. W., and Clarke, D. M. (2005) Do drug substrates enter the common drug-binding pocket of P-glycoprotein through "gates"?, *Biochem. Biophys. Res. Commun. 329*, 419−422.
34. Loo, T. W., and Clarke, D. M. (1994) Mutations to amino acids located in predicted transmembrane segment 6 (TM6) modulate the activity and substrate specificity of human P-glycoprotein. *Biochemistry 33*, 14049−14057.
35. Loo, T. W., and Clarke, D. M. (1995) Membrane topology of a cysteine-less mutant of human P-glycoprotein, *J. Biol. Chem. 270*, 843−848.
36. Loo, T. W., and Clarke, D. M. (1995) Rapid purification of human P-glycoprotein mutants expressed transiently in HEK 293 cells by nickel-chelate chromatography and characterization of their drug-stimulated ATPase activities, *J. Biol. Chem. 270*, 21449−21452.
37. Loo, T. W., and Clarke, D. M. (1994) Prolonged association of temperature-sensitive mutants of human P-glycoprotein with calnexin during biogenesis, *J. Biol. Chem. 269*, 28683−28689.
38. Loo, T. W., and Clarke, D. M. (1994) Functional consequences of glycine mutations in the predicted cytoplasmic loops of P-glycoprotein, *J. Biol. Chem. 269*, 7243−7248.
39. Loo, T. W., and Clarke, D. M. (1995) P-glycoprotein. Associations between domains and between domains and molecular chaperones, *J. Biol. Chem. 270*, 21839−21844.
40. Loo, T. W., and Clarke, D. M. (1996) Inhibition of oxidative cross-linking between engineered cysteine residues at positions 332 in predicted transmembrane segments (TM) 6 and 975 in predicted TM12 of human P-glycoprotein by drug substrates, *J. Biol. Chem. 271*, 27482−27487.
41. Goodno, C. C. (1982) Myosin active-site trapping with vanadate ion, *Methods Enzymol. 85*, 116−123.
42. Loo, T. W., and Clarke, D. M. (1997) Correction of defective protein kinesis of human P-glycoprotein mutants by substrates and modulators, *J. Biol. Chem. 272*, 709−712.
43. Loo, T. W., and Clarke, D. M. (1998) Superfolding of the Partially Unfolded Core-glycosylated Intermediate of Human P-glycoprotein into the Mature Enzyme Is Promoted by Substrate-induced Transmembrane Domain Interactions, *J. Biol. Chem. 273*, 14671−14674.
44. Loo, T. W., Bartlett, M. C., and Clarke, D. M. (2002) Introduction of the Most Common Cystic Fibrosis Mutation (Delta F508) into Human P-glycoprotein Disrupts Packing of the Transmembrane Segments, *J. Biol. Chem. 277*, 27585−27588.
45. Chifflet, S., Torriglia, A., Chiesa, R., and Tolosa, S. (1988) A method for the determination of inorganic phosphate in the presence of labile organic phosphate and high concentrations of protein: application to lens ATPases, *Anal. Biochem. 168*, 1−4.
46. Loo, T. W., and Clarke, D. M. (2000) The packing of the transmembrane segments of human multidrug resistance P-glycoprotein is revealed by disulfide cross-linking analysis, *J. Biol. Chem. 275*, 5253−5256.
47. Loo, T. W., and Clarke, D. M. (1997) Identification of residues in the drug-binding site of human P-glycoprotein using a thiol-reactive substrate. *J. Biol. Chem. 272*, 31945−31948.
48. Loo, T. W., Bartlett, M. C., and Clarke, D. M. (2004) Residues V133 and C137 in transmembrane segment 2 are close to residues A935 and G939 in transmembrane segment 11 of human P-glycoprotein, *J. Biol. Chem. 279*, 18232−18238.
49. Stenham, D. R., Campbell, J. D., Sansom, M. S., Higgins, C. F., Kerr, I. D., and Linton, K. J. (2003) An atomic detail model for the human ATP binding cassette transporter P-glycoprotein derived from disulfide cross-linking and homology modeling, *FASEB J. 17*, 2287−2289.
50. Urbatsch, I. L., Sankaran, B., Weber, J., and Senior, A. E. (1995) P-glycoprotein is stably inhibited by vanadate-induced trapping of nucleotide at a single catalytic site, *J. Biol. Chem. 270*, 19383−19390.
51. Ambudkar, S. V., Cardarelli, C. O., Pashinsky, I., and Stein, W. D. (1997) Relation between the turnover number for vinblastine transport and for vinblastine-stimulated ATP hydrolysis by human P-glycoprotein, *J. Biol. Chem. 272*, 21160−21166.
52. Martin, C., Berridge, G., Higgins, C. F., Mistry, P., Charlton, P., and Callaghan, R. (2000) Communication between multiple drug binding sites on P-glycoprotein, *Mol. Pharmacol. 58*, 624−632.
53. Loo, T. W., Bartlett, M. C., and Clarke, D. M. (2004) The drug-binding pocket of the human multidrug resistance P-glycoprotein is accessible to the aqueous medium, *Biochemistry 43*, 12081−12089.
54. Sonveaux, N., Vigano, C., Shapiro, A. B., Ling, V., and Ruysschaert, J. M. (1999) Ligand-mediated tertiary structure changes of reconstituted P-glycoprotein. A tryptophan fluorescence quenching analysis, *J. Biol. Chem. 274*, 17649−17654.

55. Rosenberg, M. F., Callaghan, R., Modok, S., Higgins, C. F., and Ford, R. C. (2005) Three-dimensional structure of P-glycoprotein: the transmembrane regions adopt an asymmetric configuration in the nucleotide-bound state, *J. Biol. Chem. 280*, 2857−2862.
56. Al-Shawi, M. K., Polar, M. K., Omote, H., and Figler, R. A. (2003) Transition state analysis of the coupling of drug transport to ATP hydrolysis by P-glycoprotein, *J. Biol. Chem. 278*, 52629−52640.
57. Chang, G. (2003) Structure of MsbA from *Vibrio cholera*: A Multidrug Resistance ABC transporter Homolog in a Closed Conformation, *J. Mol. Biol. 330*, 419−430.
58. Reyes, C. L., and Chang, G. (2005) Structure of the ABC transporter MsbA in complex with ADP.vanadate and lipopolysaccharide, *Science 308*, 1028−1031.

BI050705J